

UC Irvine

UC Irvine Previously Published Works

Title

Solution and Interface Aggregation States of Crotalus atrox Venom Phospholipase A2 by Two-Photon Excitation Fluorescence Correlation Spectroscopy †

Permalink

<https://escholarship.org/uc/item/7kh752nc>

Journal

Biochemistry, 40(23)

ISSN

0006-2960

Authors

Sanchez, Susana A

Chen, Yan

Müller, Joachim D

et al.

Publication Date

2001-06-01

DOI

10.1021/bi001599i

Copyright Information

This work is made available under the terms of a Creative Commons Attribution License, available at <https://creativecommons.org/licenses/by/4.0/>

Peer reviewed

Solution and Interface Aggregation States of *Crotalus atrox* Venom Phospholipase A₂ by Two-Photon Excitation Fluorescence Correlation Spectroscopy[†]

Susana A. Sanchez, Yan Chen, Joachim D. Müller, Enrico Gratton, and Theodore L. Hazlett*

Department of Physics, Laboratory for Fluorescence Dynamics, University of Illinois at Urbana-Champaign, 1110 West Green Street, Urbana, Illinois 61801

Received July 11, 2000; Revised Manuscript Received April 9, 2001

ABSTRACT: The dimeric *Crotalus atrox* venom PLA₂ is part of the secreted phospholipase A₂ (PLA₂) enzyme family that interacts at the lipid–solution interface to hydrolyze the *sn*-2 acyl ester bond of phospholipids. We have employed fluorescence correlation spectroscopy (FCS) to study the monomer–dimer equilibrium of the *C. atrox* venom PLA₂ in solution, in the presence of urea, and in the presence of monomeric and micellar *n*-dodecylphosphocholine (C12-PN), a phosphatidylcholine analogue. Dilution experiments show that PLA₂ is an extremely tight dimer, $K_d \leq 0.01$ nM, in solution. Urea was introduced to weaken the subunit's association, and an estimate for the PLA₂ dimer dissociation constant in buffer was obtained by linear extrapolation. The derived dissociation constant was at least several orders of magnitude greater than that suggested from the dilution experiments, indicating a complex interaction between urea and the PLA₂ dimer. FCS data indicate that the PLA₂ dimer begins to dissociate at 10 mM C12-PN in 10 mM Ca²⁺ and at 5 mM C12-PN in 1 mM EDTA. The PLA₂ tryptophan fluorescence displayed spectral shifts and intensity changes upon interacting with C12-PN. On the basis of the FCS and tryptophan fluorescence results, we postulate an intermediate state where the two monomers are in loose interaction within a protein–lipid comicelle. As the concentration of C12-PN was increased, complete dissociation of the dimer was observed, inferred from the doubling of the particle number, and the average diffusion constant decreased to approximately 60 μm²/s, consistent with PLA₂ associated with a C12-PN micelle. The presence of Ca²⁺ makes the comicelle intermediate more stable, retarding the separation of the monomers in the micellar suspension. Our data clearly indicate that PLA₂, though a strong dimer in the absence of lipids, is dissociated by micellar C12-PN and supports the monomer hypothesis for PLA₂ action.

Secreted phospholipase A₂'s (PLA₂)¹ constitute a family of calcium-dependent enzymes which hydrolyze the *sn*-2 acyl ester bond of phospholipids. They may be isolated from the pancreas and snake or insect venoms, and some forms have now been cloned. Their primary structures are similar with 50–70% sequence homology, and their monomer molecular masses range from approximately 13 to 15 kDa. The secreted PLA₂'s are soluble enzymes that interact at the solution–lipid interface of micellar and bilayer phospholipids to hydrolyze phospholipid into lysophospholipid and free fatty acid.

The interactions of PLA₂s with lipids have been extensively studied over the last 30 years. The focus of these studies has been on the effect of lipid organization on enzymatic activity (1–3). The PLA₂ specific activity against monomeric phospholipids is poor but is greatly enhanced,

from 10- to 100-fold, when the lipid is organized in micellar form (4). Under the appropriate conditions, PLA₂ interfacial activation in phospholipid bilayers can be observed as a delay period before the onset of active phospholipid hydrolysis (5, 6). Researchers exploring the nature of the lag phase events have implicated several factors which seem to be critical in this process, including the fluctuation of lipid microdomains (7–9), the extent of membrane curvature (10, 11), and the overall charge of the lipid membrane. Early in PLA₂ research, it was noted that some PLA₂s were dimeric in solution, which lead several groups to propose that interfacial activation of monomeric forms involves dimer formation (12–17). In fact, calcium, an essential cofactor for activity, has been proposed to favor protein dimerization for some PLA₂s (18–20). Considering the similarity in sequence and catalytic mechanism within this group of enzymes, it would appear that the monomer contains all of the necessary structure for full enzymatic activity. However, the existence of tight dimer PLA₂s such as the PLA₂ from *Crotalus atrox* venom begs the question as to the role that the dimer plays in PLA₂ function. Whether or not the dimer is the active form remains an unanswered question with sporadic support appearing in the literature (5, 13). Thus, our interest in the monomer–dimer equilibrium of the *C. atrox* PLA₂ stems from specific questions about the influence of the dimer on function, i.e.,

[†] This work was supported by grants from the NIH (RR03155) and the American Heart Association (IL 97-CGS-07/G10).

* To whom correspondence should be addressed. Phone: 217-244-5620. Fax: 217-244-7187. E-mail: thazlett@uiuc.edu.

¹ Abbreviations: PLA₂, phospholipase A₂; FCS, fluorescence correlation spectroscopy; CMC, critical micelle concentration; C12-PN, *n*-dodecylphosphocholine; Fluo-PLA₂, fluorescein-labeled PLA₂; Laurdan, 6-dodecanoyl-2-(dimethylamino)naphthalene; C14-PN, *n*-tetradecylphosphocholine; C16-PN, *n*-hexadecylphosphocholine; EDTA, (ethylenedinitrilo)tetraacetic acid; GL, 3-D Gaussian–Lorentzian model.

the original active dimer (and half-the-sites) hypotheses presented in earlier works (15) or involvement with the lag/burst phase kinetics (5), but also from general questions on protein–protein interactions and protein interactions with a membrane interface.

Early studies on the *C. atrox* venom PLA₂ quickly identified this enzyme as a strong dimer, similar to another dimeric PLA₂ isolated from *Crotalus adamanteus* venom (21–23). The secreted PLA₂ from *C. atrox* is a dimer when free in solution (20) with a reported K_d in the nanomolar range (24). Using chromatographic profiles, Myatt et al. also studied the effect of Ca²⁺ on the K_d , and they report a 8-fold decrease of the dissociation constant when the cofactor is present. Hydrolysis activity studies on the strong dimer PLA₂s indicated that the active unit was likely a dimer with a dissociation constant of 0.6 nM in the presence of lipid substrate and Ca²⁺ cofactor (21). Other researchers have questioned the general conclusions and began examining monomeric PLA₂s and searching for ways to identify the active unit in the presence of substrate (18, 19, 25, 26).

A common experimental observation has been reported for PLA₂s when they interact with lipid interfaces: changes in tryptophan emission (5, 6, 27, 28). In studies on micellar lipid interactions with PLA₂s, at lipid concentrations below the CMC (critical micellar concentration), small decreases in the tryptophan emission may occur depending on the enzyme source and pH (29). At lipid concentrations above their CMC there is normally an increase in tryptophan emission accompanied by a blue shift of the emission maximum (29). This increase in tryptophan fluorescence has been attributed to direct lipid–protein interactions, conformational changes in the enzyme/lipid complex, and, the most controversial one, postulated changes in the aggregation state of the enzyme. Direct biophysical studies to determine the aggregation state of this enzyme when interacting with lipids in any of its conformations (micelles, bilayers, etc.) have been rare. Hydrolysis data by Jain and co-workers suggest that *C. atrox* venom PLA₂ is a dimer in solution but dissociates at the lipid interface, but no physical evidence has been forthcoming. In contrast, a recent report by Ferreira et al. on immobilized PLA₂ from *C. atrox* venom identified this enzyme as an active dimer (13).

Few techniques can be applied onto a membrane or micelle surface. One of the most commonly used fluorescence techniques in studying oligomer dissociation is fluorescence polarization (30–32). The ratio of the rotational correlation time of the dimer to the monomer is 2, due to the volume change, which allows studying monomer/dimer equilibrium in solution for small proteins. However, in the PLA₂ case in which the dimer dissociates upon interaction with lipids, there is an additional change in mass due to the number of lipids that associate with the protein. Thus, fluorescence polarization cannot be used to study dimer dissociation under this condition.

An alternative fluorescence technique that can provide information about monomer/dimer equilibrium and, at the same time, determine the mass of the protein/lipid aggregates is fluorescence correlation spectroscopy (FCS). This technique allows one to count the number of fluorophore-labeled proteins in a particle aggregate using the fluctuation of the fluorescence intensity. The fluctuation amplitude is inversely proportional to the number of particles in the excitation

volume for a single molecular species. In our case, a decrease in the fluctuation amplitude, $G(0)$, by a factor of 2 will indicate complete dissociation of the PLA₂ (33). An additional advantage of the FCS techniques is the very high sensitivity permitting its use at very low protein concentrations (subnanomolar range), which is crucial for the present study.

In this work, we have determined an upper limit for the K_d by dilution of the enzyme through at least 3 orders of magnitude in concentration, in the presence and absence of Ca²⁺. We also studied the effect of urea on the dissociation of the enzyme. In the presence of urea the enzyme dissociates without being denatured (as reported by the CD signal at 220 nm). We also studied the interaction of PLA₂ with lipids to answer specific questions as to the state of the enzyme (monomeric vs dimeric) below and above the CMC of the C12-PN lipid analogue. Since we were independently following the dissociation of the enzyme using FCS, we were also able to determine whether there is correlation between the changes in tryptophan emission with enzyme dissociation. We measured the number of enzyme particles when lipid monomers are present (below the CMC) and when micelles are already formed (above the CMC). The comparison of dissociation curves of the number of particles and of tryptophan emission at different lipid concentrations in the presence and absence of Ca²⁺ allowed us to address the above questions and to propose a structural model for PLA₂/lipid interactions. Most importantly, our data indicate that the PLA₂ dimer dissociates into monomers given sufficient micellar lipid and suggest that under assay conditions and in the presence of substrate the monomer form is the active enzyme form.

Finally, this study shows that extending traditional fluorescence measurements to FCS can be a promising approach to study the interaction of protein in its natural biological environment (interacting with lipids). Here, FCS provides a direct measure of the dissociation process, while conventional fluorescence probes environmental factors affecting the chromophore. The combination of both techniques provides complementary information that allows us to formulate a more detailed model.

MATERIALS AND METHODS

Sample Preparation. The PLA₂ from *C. atrox* venom (Miami Serpentarium, Punta Gorda, FL) was purified in our laboratory using standard methods (34). Fluorescein conjugates of PLA₂ were prepared with fluorescein succinidyl ester (Molecular Probes, Eugene, OR) using standard methodology. Laurdan was purchased from Molecular Probes ((Molecular Probes, Eugene, OR). The labeled fluorescein/enzyme ratio was calculated using an extinction coefficient for fluorescein of $\epsilon_{499} = 70\,000\text{ M}^{-1}\text{ cm}^{-1}$ (35), and the protein concentration was determined using either Bio-Rad Protein Assay (Bio-Rad, CA) for the labeled enzyme or $\epsilon_{280} = 25\,000\text{ M}^{-1}\text{ cm}^{-1}$ (34) for the enzyme without labeling. Enzymatic activity was measured in a pH-stat using a mixed micelle assay at pH = 8.0 (36). The labeling ratio 2 fluoresceins per protein and the enzyme conjugates retained >90% of the activity of unlabeled PLA₂. The phospholipid analogue *n*-dodecylphosphocholine was from Avanti Polar Lipids (Alabaster, AL). Urea and general chemicals were from Fisher Scientific (Fair Lawn, NY).

FCS Experiments. The instrumentation for two-photon fluctuation experiments is similar to that described by Berland et al. (37) with the following modifications: the experiments were carried out using a Zeiss Axiovert 135 TV microscope (Thornwood, NY) with a 63X Plan Apochromat-oil immersion objective (NA = 1.4). A mode-locked Ti:sapphire laser (Mira 900; Coherent, Palo Alto, CA) pumped by an intracavity doubled Nd:YVO₄ vanadate laser (Verdi; Coherent Inc., Santa Clara, CA) was used as a two-photon excitation source. For all measurements, an excitation wavelength in the range from 770 to 780 nm was used, while the average power at the sample ranged from 7 to 2 mW. Photon counts were detected using an Avalanche photodiode detector (APD) (Model SPCM-AQ-151; EG&G). The output of the APD unit was directly connected to the data acquisition card. The photon counts were sampled at either 20 or 100 kHz. The recorded photon counts were later analyzed with programs written in PV-WAVE version 6.10 (Visual Numerics). Samples were mounted in a sample holder fabricated out of Delring (Illini Plastic, IL). A drilled hole in the center of the chamber was covered by a 1.5 mm standard microscope cover glass and used as the window for the microscope objective. There were no additional treatments applied to the Delring or cover glass surfaces. The holder was extensively cleaned between each measurement.

(A) Dilution Experiments. In the dilution experiments, the sample holder was placed in the microscope, coupled with immersion oil, and kept there until the last sample was measured. Three sets of samples were measured: fluorescein, fluorescein-PLA₂ (Fluo-PLA₂) in 1 mM EDTA, and Fluo-PLA₂ plus 10 mM CaCl₂ in 50 mM Tris, pH 8.0. A fluorescein standard was used to calibrate the equipment. Each series of measurements started by the buffer alone, then the Fluo-PLA₂ was diluted from a concentrated stock to the initial concentration of the set, and all the following dilutions were done in the same cuvette. Adsorption of molecules to the container walls is a concern when performing titration experiments at low concentrations. To ensure that adsorption did not influence our results, we performed the experiments in both directions: starting from either low or high PLA₂ concentrations. The results were independent of the protocol, indicating that PLA₂ adsorption did not adversely affect our studies.

(B) Dissociation with Urea. The samples, at different concentrations of urea, were prepared and incubated overnight. Protein concentration was kept constant at 0.1 μM. The sample holder was also kept in place until the last sample was measured. In this case after each sample was measured, the cuvette was washed with buffer several times until the fluorescence reached the background counts of the buffer. In this type of experiment we also used fluorescein at the same urea concentrations as a control.

(C) Lipid-PLA₂ Interactions. Independent samples with different *n*-dodecylphosphocholine (C12-PN) concentrations in 50 mM Tris, pH 8 (with or without Ca²⁺), were prepared, and the fluorescently labeled enzyme was added. Protein concentration was kept constant at 0.14 μM. The chamber was also washed exhaustively with buffer between samples.

PLA₂ Emission Spectra. Tryptophan emission spectra were recorded between 310 and 450 nm, with excitation at 295 nm on a Fluoromax-2 (JOBIN YUON-SPEX, Instruments S.A., Inc., Edison, NJ) connected to a water bath at 25 °C.

Protein concentration was 0.14 μM, unless otherwise stated. Unlabeled protein was used to avoid any quenching of the signal due to energy transfer between the tryptophan and fluorescein. For each emission spectrum, two parameters were calculated: the center of mass and the total area of the emission band.

CD Spectra. Circular dichroism spectra were taken on a JASCO J-720 spectropolarimeter. Spectra were obtained for PLA₂ under varying concentrations of urea at a protein concentration of 14 μM in Tris buffer, pH 8. Samples were incubated with denaturant overnight before the spectra were collected. Each spectrum was obtained at 25 °C in a 0.1 cm optical path cell. Wavelengths were scanned between 250 and 190 nm at 50 nm/min with a band-pass of 0.5 nm.

FCS Data Analysis. Experimental autocorrelation functions were fitted with an equation assuming a Gaussian-Lorentzian intensity profile, as described in a previous work which contains the explicit formulas for the point spread function and the definition of the beam waist used (37). The beam waist of the Gaussian-Lorentzian function depends on the instrument setup and must be calibrated each time the system is aligned. For this purpose a substance with a known concentration and diffusion coefficient (*D*) was used to calibrate the excitation volume. In this work, fluorescein (in 50 mM Tris, pH 8.0), with a reported diffusion constant of 300 μm²/s (33), was used as the standard. The recovered beam waist value of 0.37 μm was used to perform a global analysis with each set of data (dilution, urea, etc.). For a single species, the fluctuation amplitude, *G*(0), is related to the number of particles by

$$G(0) = \gamma/\bar{N} \quad (1)$$

where \bar{N} is the average number of molecules inside the excitation volume and γ is a geometric factor that is only determined by the shape of the point spread function, determined by the mathematical model used and the determined width parameters. The geometric factor for the Gaussian-Lorentzian model is 0.0762 (38). For a mixture of species, the *G*(0) value is related to the number of molecules of the individual species by (33)

$$G(0) = \sum_{m=1}^M \left(\frac{\langle F_m \rangle}{\langle F_T \rangle} \right)^2 G_m(0) \quad (2)$$

where $\langle F_T \rangle$ and $\langle F_m \rangle$ are the average fluorescence intensities of the overall mixture and the individual species, respectively, and *M* is the total number of species.

The *G*(0) value was corrected for the buffer contribution by extending eq 2 for two species as shown in the equation:

$$G_{\text{measured}}(0) = \left(\frac{\langle F_{\text{sample}} \rangle}{\langle F_T \rangle} \right)^2 G_{\text{sample}}(0) + \left(\frac{\langle F_{\text{buffer}} \rangle}{\langle F_T \rangle} \right)^2 G_{\text{buffer}}(0) \quad (3)$$

where the fluorescence intensity of the buffer, F_{buffer} , and the *G*(0) value of the buffer, $G_{\text{buffer}}(0)$, can be determined independently by performing FCS experiment on the buffer. $G_{\text{measured}}(0)$ is extrapolated by the experimental autocorrelation function, and F_{sample} is the fluorescence intensity of the sample of interest and is equal to $\langle F_T \rangle - \langle F_{\text{buffer}} \rangle$. For our

experiments, the $G_{\text{buffer}}(0)$ is 9.5 and F_{buffer} is 240 cps (counts per second), respectively.

We obtained the extrapolated $G(0)$ and the diffusion coefficient, for each sample in a series, by fitting the experimental autocorrelation function to eq 3. For a mixture of species, the recovered diffusion constant reflects the average diffusion constant of the mixture. The $G(0)_{\text{sample}}$ when multiple species are present, such as the dimeric and monomeric forms of PLA₂, gives an apparent number of particles weighted by the $G(0)$ s and fractional contributions of each specie. Once the protein is fully dissociated, only the monomeric species is present and the fluctuation amplitude characterizes again the true number of particles.

The standard deviations for D and $G(0)$ were obtained by collecting a large single data stream and dividing it into 10 separate sets consisting of 9000–13 000 kB each. The resolved values and their associated errors were subsequently calculated from the independent fits to the 10 data sets. However, experimental uncertainties due to different instrument setup, optical alignment, and sample preparation from day to day, gave larger contributions to the point-to-point variations than the statistical error (Figure 3).

Dimer–Monomer Equilibrium. According to classical chemical thermodynamics, the equilibrium of dimer and monomers admits a single dissociation constant K_d related to α , the degree of dissociation of the dimer, by the expression:

$$K_d = \frac{4\alpha^2 C}{1 - \alpha} \quad (4)$$

where C is the total protein concentration in terms of the protein dimer. In logarithmic form:

$$\log \frac{K_d}{4C} = \log \left[\frac{\alpha^2}{(1 - \alpha)} \right] \quad (5)$$

The plot of degree of dissociation α against $\log C$ has a characteristic span of 2.86 decimal logarithmic unit between $\alpha = 0.1$ and $\alpha = 0.9$ (39, 40).

RESULTS

K_d Estimation by Dilution. To determine the solution dissociation constant for the *C. atrox* PLA₂ dimer, we have measured the number of fluorescent particles in the excitation volume using the fluctuation amplitude in the FCS experiment (eq 1) as we dilute the enzyme solution. Figure 1 shows typical autocorrelation curves obtained in this study. They were measured for fluorescein (used for instrument calibration) and Fluo-PLA₂. The diffusion coefficient obtained for the protein was $75 \mu\text{m}^2/\text{s}$. The $G(0)$ was normalized in this figure but will depend on the protein concentration at each point of the dilution process. In Figure 2, the number of particles multiplied by the dilution factor is plotted versus concentration. In this plot, a straight line indicates that the number of molecules changes in proportion with the dilution. If there is dissociation, a deviation from the straight line will be observed. For the control experiment (dilution of fluorescein in 50 mM Tris, pH 8.0, 1 mM EDTA), we observed a straight line down to 1.5×10^{-10} M (open squares). This is the expected result since fluorescein does not self-

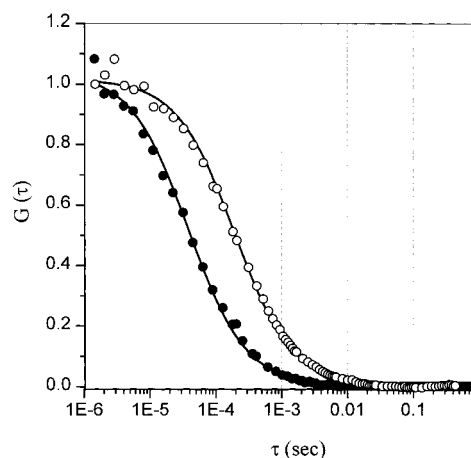


FIGURE 1: Normalized autocorrelation curve $G(\tau)$. Normalized autocorrelation for data taken at 100 kHz for fluorescein (filled circles) and fluorescein-labeled PLA₂ (open circles). Curved lines correspond to the best fit parameters (see Materials and Methods). $G(0)$ values have been normalized, and the instrument was calibrated with fluorescein using a diffusion coefficient of $300 \mu\text{m}^2/\text{s}$. The dimer PLA₂ data were best fit to a diffusion coefficient of $75 \mu\text{m}^2/\text{s}$.

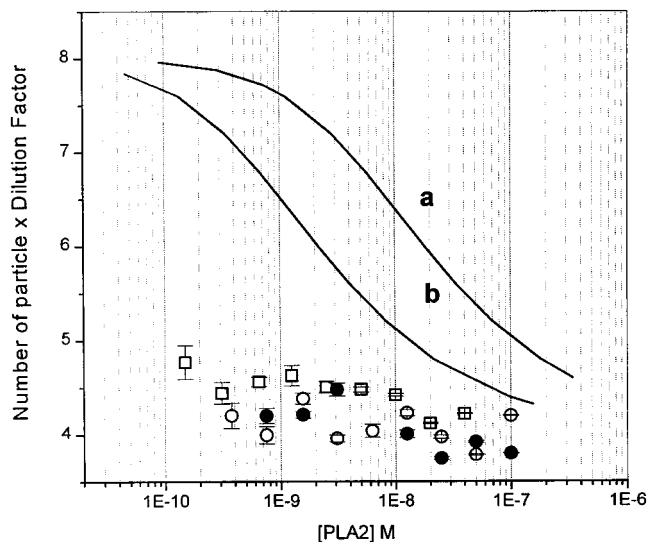


FIGURE 2: Changes of particle number with dilution. Samples of fluorescein-labeled *C. atrox* PLA₂ have been diluted in the absence (open circles) and in the presence of 10 mM Ca²⁺ (filled circles) in 50 mM Tris, pH 8. Fluorescein in the same buffer was used as a control (open squares). The number of particles was calculated from the $G(0)$, and the number of particles multiplied by the dilution factor was plotted against protein concentration (in terms of monomer concentration). For reference, simulation curves are shown for dissociation constants of 36 (a) and 4.3 nM (b).

aggregate nor stick to the surfaces of our sample holder, so the number of particles changes exclusively due to the dilution. When the Fluo-PLA₂ was diluted, we observed a straight line in the analysis plot (Figure 2). The addition of 10 mM calcium did not change the scenario: the number of molecules decreased proportionally with the dilution, indicating that the PLA₂ dimer remained intact. Using eq 4, we calculated that the maximum value of K_d compatible with these data would be in the 0.01 nM range. Assuming a K_d value, a simulated curve can be drawn that represents the hypothetical dissociation pattern in a given concentration range. In Figure 2, two simulations are shown for K_d values equal to 36 nM and 4.3 nM labeled as a and b, respectively.

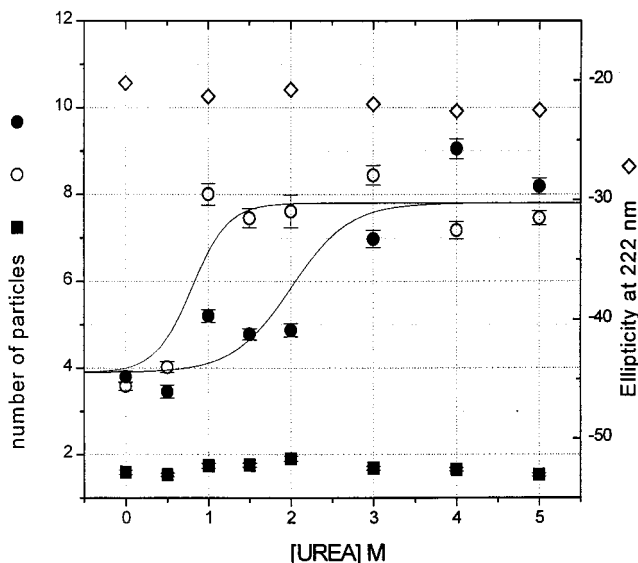


FIGURE 3: The number of particles (Fluo-PLA₂, monomers and dimers) are given as a function of urea concentration. Independent samples of constant enzyme concentration (0.1 μ M) and increasing urea concentration were prepared in 50 mM Tris, pH 8, in the absence (1 mM EDTA) (open circles) and in the presence of 10 mM Ca²⁺ (filled circles). Fluorescein in the same buffer was used as a control (filled squares). The CD signal at 222 nm for each urea concentration is also shown (open diamonds).

These K_d values correspond to those reported in the literature for the dissociation constant in the absence and in the presence of Ca²⁺ (24).

Urea was used as an external agent to dissociate the PLA₂ dimer. The number of fluorescent particles in the excitation volume at different concentrations of urea is shown in Figure 3. Again fluorescein was used as a control (filled squares), and the number of molecules did not change with increasing concentration of denaturant. In the case of the PLA₂ dimer in the presence (filled circles) and absence (open circles) of calcium, the number of molecules in the excitation volume changed from 4 to 8. However, the concentration ranges where these changes occur are different. When calcium is present, the changes occur between 1 and 3.5 M with a middle point around 2.0 M urea. In the absence of calcium, the middle point occurs at a lower concentration, 0.8 M urea.

For each concentration of urea an apparent K_d was calculated using eq 4. We used the method proposed by Santoro and Bolen (41) to extrapolate the dissociation constants at high urea concentration to zero urea concentration. We obtained extrapolated K_d values of 3.5 nM for the dissociation in the absence of calcium and 0.63 nM when calcium was present. Figure 3 also shows the CD signal at 222 nm obtained for PLA₂ at different urea concentrations (open diamond). No variation of the CD signal was observed until 6 M urea. Table 1 summarizes the K_d for the extrapolated values from urea experiments, the estimated values obtained in the dilution experiments, and values previously reported in the literature (24).

PLA₂-Lipid Interactions. We measured three parameters, (a) center of mass (squares), (b) area of the tryptophan emission peak (crosses), and (c) number of particles in the excitation volume (filled circles), to study the interaction of *C. atrox* PLA₂ with the lipid analogue *n*-dodecylphosphocholine (C12-PN) in the absence and presence of 10 mM

Table 1: Solution Dissociation Constants for *C. atrox* PLA₂

	conditions	K_d (nM)
FCS dilution experiments	1 mM EDTA	≤ 0.01
	10 mM Ca ²⁺	≤ 0.01
FCS urea dissociation ^a	1 mM EDTA	3.5
	10 mM Ca ²⁺	0.63
chromatography ^b	1 mM EDTA	36
	10 mM Ca ²⁺	4.3

^a Dissociation constant obtained using FCS results and the linear extrapolation method. ^b Data reported by Myatt et al. (24).

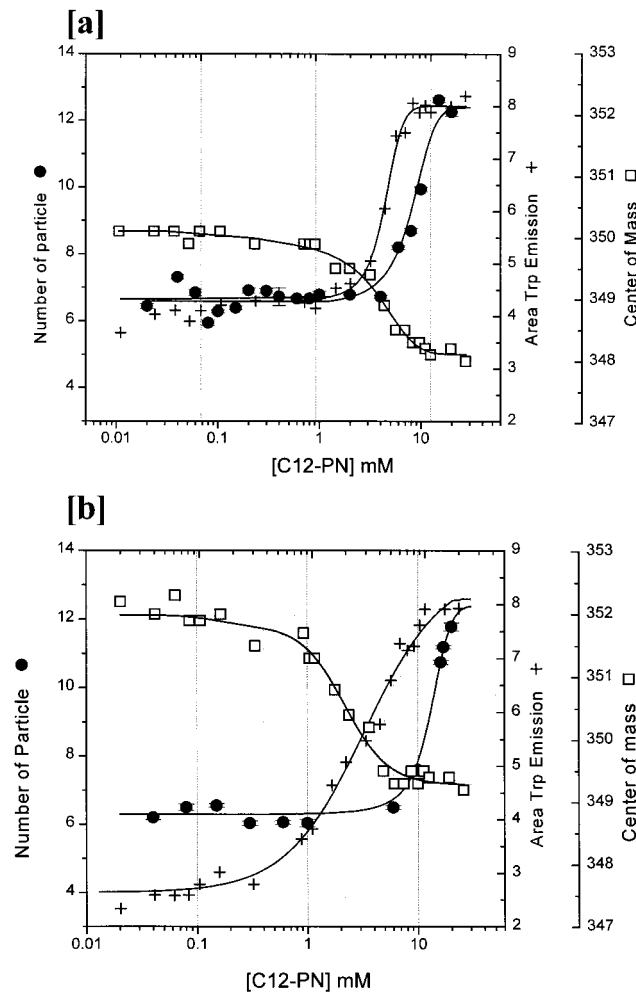


FIGURE 4: *C. atrox* PLA₂ and *n*-dodecylphosphocholine association. Area (crosses) and center of mass (squares) for tryptophan emission and the number of particles (filled circles) of *C. atrox* PLA₂ interaction C12-PN. The enzyme concentration was held constant at 0.14 μ M. Samples were prepared in 50 mM Tris, pH 8, buffer and 1 mM EDTA (a) or in 10 mM Ca²⁺ (b), and the measurements were performed at 20 °C.

Ca²⁺ (Figure 4). The number of PLA₂ particles in the excitation volume (filled circles) behaves similarly in the presence or absence of Ca²⁺ and increases from 6 to 12 as a function of lipid analogue concentration. However, the concentration range where the changes occurred depended on the presence of Ca²⁺. In the absence of calcium, the range spanned from 6 to 20 mM with a middle point at 8 mM. In the presence of 10 mM Ca²⁺ the range becomes larger, from 2.5 to 20 mM, and the middle point moves up to 10.5 mM. At 20 mM lipids the PLA₂ dimers were completely dissociated in both cases.

Table 2: Diffusion Coefficients ($\mu\text{m}^2/\text{s}$)^a for the Fluo-PLA₂, C12-PN Micelles, and Fluo-PLA₂/C12-PN Mixtures^b

C12-PN (mM)	1 mM EDTA	10 mM calcium
0	75	75
0.04	73	75
0.08	71	
0.15	72	72
0.2	73	
1	72	75
6	71	
8	70	
10	78	71
16		60
19	65	
20	60	55
C12PN micelles ^c	57	

^a Obtained from the fitting of the autocorrelation function as described in Materials and Methods. Errors in the diffusion constants were estimated to be no greater than 10%. ^b 50 mM Tris, pH 8. ^c C12-PN micelles (10 mM) containing Laurdan.

In addition to the particle number, the diffusion constant of the particle gives a measure of the extent of C12-PN association with PLA₂. The diffusion constant of Fluo-PLA₂ as a function of C12-PN concentration is given in Table 2. At monomer C12-PN concentrations [below the CMC of 1.1 mM (42)] the particle diffusion constant was found to be approximately 72 $\mu\text{m}^2/\text{s}$, similar to the value found for the PLA₂ dimer, 75 $\mu\text{m}^2/\text{s}$. As the concentration of C12-PN was increased above the CMC, both in the presence and in the absence of Ca²⁺, the diffusion constant progressively decreased, indicating an increase in particle size. At 20 mM C12-PN a diffusion constant of 60 $\mu\text{m}^2/\text{s}$ (55 $\mu\text{m}^2/\text{s}$ in the presence of Ca²⁺) was reached. The diffusion constant for micellar C12-PN was obtained through the collection of FCS data on Laurdan-containing micelles and was found to be 57 $\mu\text{m}^2/\text{s}$ (Table 2).

The area of the tryptophan emission spectra also changed when C12-PN was added. The final intensity for the two cases studied, with and without Ca²⁺, was the same, but the starting point was lower in the presence of Ca²⁺. The fluorescence increase in both cases followed a sigmoidal behavior. In the presence of EDTA, the spectral changes occurred in the lipid concentration range between 1 and 10 mM with a middle point at 4.5 mM. In contrast, when calcium was added, the range was larger, from 0.3 to 20 mM, and the middle point was near 3 mM C12-PN.

The center of mass of tryptophan emission spectra is another marker of lipid/protein interaction. A blue shift of tryptophan emission spectra was observed upon lipid titration in both cases, in the presence and absence of Ca²⁺. The plateau of the blue shift was observed around 20 mM in both cases with a value of 349.5 and 348.0 nm in the presence and absence of 10 mM Ca²⁺, respectively.

DISCUSSION

The primary focus of this work is on the dimer–monomer equilibrium of the strong dimer PLA₂ from *C. atrox* venom. To determine the dissociation constant, we used an approach based on the fluctuation correlation spectroscopy technique. This technique is capable of determining the number of fluorescent particles in the excitation volume (approximately 0.1 fL in our instrument) and the diffusion coefficient of

the particles. In this way, we were able to determine the aggregation state of the protein (monomer vs dimer) in the presence of denaturant and in the presence of lipids. Our work constitutes a significant advance because we were able to follow directly the dissociation of dimer PLA₂ in solution, in the presence of lipid monomers and lipid micelles. The determination of the dissociation of the enzyme has historically been a difficult task since the PLA₂ subunit affinity is high and the protein needs to be diluted several orders of magnitude to accurately determine the dissociation constant (39, 43). At each point of the dilution, we must measure a property which can distinguish monomer from dimer. The first experimental problem generally encountered is the sensitivity of a technique for measuring the desired property. The tighter the dimer, the more challenging it is to find an adequately sensitive technique. Fluorescence spectroscopy is one of the more sensitive spectroscopic methodologies commonly applied to studies on binding equilibria. In fact, fluorescence methods can achieve single molecule detection levels. In some systems the intrinsic protein fluorescence can be used, but tryptophan fluorescence, the primary protein fluorophore, is not strong enough for measuring K_d values much below 10⁻⁸ M. For high sensitivity such as this work, extrinsic fluorophores must be used.

A second consideration in studying binding equilibria is that the chosen method must adequately distinguish monomer from dimer. Fluorescence polarization is commonly used to study aggregation equilibria in proteins. Polarization measurements are based on the changes in particle hydrodynamic volume during protein dissociation (32, 43, 44). Although dependent on the particle shape, the ratio between dimer and monomer rotational correlation times should be approximately 2. This technique can be applied to solution studies, but it cannot be easily applied for our specific case in which the changes in the association state of PLA₂ are accompanied by changes in the interaction of PLA₂ with organized lipids. For example, in our condition in which the PLA₂ begins associating with lipids and simultaneously dissociating from dimer to monomer, there would be an increase in the hydrodynamic volume due to lipid binding (in the form of monomers, micelles, or vesicles) but a decrease in the volume due to the dissociation of the dimer. In this scenario we would observe an average polarization change, a distribution of rotational correlation times, which would be difficult to accurately interpret. In contrast, fluorescence correlation spectroscopy will not only give us the sensitivity, which we expect from fluorescence techniques, but also allows us to detect dissociation in terms of the number of molecules in the excitation volume. If a dimer dissociates into its monomers, the number of fluorescent molecules in the excitation volume will increase by a factor of 2 due to dissociation (dimer to monomer). The upper concentration in the FCS experiments is determined mainly by the fluctuation amplitude, $G(0)$. The inverse relation between the number of molecules in the excitation volume $\langle N \rangle$ and $G(0)$ indicates the importance of limiting the number of molecules inside the excitation volume to observe appreciable fluctuations. If the volume of excitation contains many molecules, the average intensity will fluctuate very little. The lower concentration limit in the fluorescence fluctuation spectroscopy experiments is imposed by the signal-to-noise ratio, which in our case is determined by the fluorescence

contribution from the buffer. The fluorescence intensity of the buffer is relatively high when compared to water. Therefore, it is important for the more diluted samples that we take the buffer contribution into account (eq 2).

The effect of pH and Ca²⁺ on the binding constants has been previously studied using chromatographic profiles (24). By examining the width and position of the gel filtration profiles, the authors estimated that the K_d is approximately 36 nM and 4.3 nM in the absence and presence of Ca²⁺, respectively. From our dilution data, no dissociation is observed. The enzyme K_d , according to our calculation, would be on the order of 0.01 nM. Plotting our data and the simulated curves using their K_d values (Figure 2) shows obvious disagreement.

The discrepancy between our data and the reported values might be explained by the nature of the PLA₂. The phospholipases A₂ are surface-active proteins. Techniques such as gel filtration rely on the assumption that the protein does not associate with the column matrix. Any interaction will drive the protein to longer retention times and lower apparent molecular weights. These effects are particularly troublesome at low protein concentrations. It is also true that these techniques are carried out under nonequilibrium conditions, which can also influence the results. In contrast, in FCS one collects data on a protein solution under equilibrium conditions. However, we must acknowledge that we have an extrinsic label attached to the PLA₂ which may alter the monomer–dimer equilibrium. We believe our conjugate is well behaved since its activity appears normal against micellar substrate, and modifications would generally be thought to disrupt specific interactions, not enhance them.

The use of reagents such as urea to weaken the molecular interactions is a common tool in oligomer biochemistry. The problem associated with using these types of reagents is that it is possible to denature the protein subunits as well as perturb the oligomer equilibrium (32). The fact that the CD signal does not change in the range of urea concentrations used indicates that at least the secondary structure of the protein was unaffected. The stability of PLA₂ in urea has been reported by others, and it is not a surprising result, since *C. atrox* venom PLA₂ contains seven sulfur bridges per monomer which greatly stabilize the subunit structure (45).

We explored the possibility of obtaining indirectly the K_d values using the “linear extrapolation method” (41) from urea dissociation experiments. This methodology is normally used in denaturation studies to calculate the stabilization free energy of the folded state by extrapolation of the denaturant-unfolded state’s free energies to zero denaturant concentration. The assumption for the application of this methodology is the existence of two states, native (N) and unfolded (U) in equilibrium, with a constant K_{denat} and that urea does not directly participate in the equilibrium. In the case of a monomer–dimer equilibrium we have two states, monomer and dimer, with a single equilibrium constant, K_d . We calculate the extrapolated K_d in the presence ($K_d = 0.63$ nM) and in the absence of 10 mM Ca²⁺ ($K_d = 3.5$ nM), which indicates that Ca²⁺ increases the dimer stability. However, the extrapolated K_d values are not compatible with the upper limit obtained from the direct dilution experiments, indicating that urea participates in a complex manner. An interesting work published by Weber’s group some years ago studied the pressure dissociation of the R17 bacteriophage (46). They

reported a different dissociation pattern when urea was used to facilitate the dissociation compared with pressure-induced dissociation in the absence of urea. The authors concluded that urea loosens the interaction between the monomers, but at the same time it fundamentally changed the interfacial binding sites. Their work, and the work presented here, suggests that care must be taken using these extrapolation methods in determining free energies for even relatively well-defined two-state processes.

Changes in the tryptophan emission when PLA₂ interacts with organized lipid structures, such as micelles, have been reported. The question is whether these changes are related or not with the dissociation of the enzyme. *C. atrox* PLA₂ has six tryptophans (45), three tryptophan residues per subunit, two of which are located near the surface of the molecule. The third one is located near the calcium binding site, protected from the solvent by the companion PLA₂ subunit. It is well-known that tryptophan emission can be affected by the polarity of the surroundings. Spectral blue shift is characteristic when the tryptophan environment becomes less polar (47). Given the number of the tryptophans present, the spectral shift and intensity changes cannot be unambiguously assigned to specific residues in the protein.

Unlike the tryptophan emission, the fluctuation amplitude measured by FCS derives from fluorescein molecules covalently bound to the protein. The fluctuations, as outlined in the Materials and Methods section, can give us information about the dissociation state of the molecule. In this way, the combination of tryptophan signal and the measurement of the number of molecules in the excitation volume gives us a handle to separate the effects of protein dissociation from protein/lipid interactions.

On the basis of our combined FCS and tryptophan fluorescence results, we propose the following model based on four states for the interactions of *C. atrox* PLA₂ dimer with lipid micelles in the absence and presence of Ca²⁺ (Figure 5).

State a: In the absence of lipids, the enzyme is a dimer and remains in this state until at least 10⁻¹¹ M according to our dilution studies. The addition of calcium at this stage produces an increase in intensity and a red shift (Figure 4) of the tryptophan emission spectra. Even if the changes in tryptophan intensity represent the average behavior of all the six tryptophans in the dimer protein, we can assume that the changes produced after the addition of Ca²⁺ are due to Ca²⁺ binding to the enzyme’s active site.

State b: C12-PN below its CMC of 1.1 mM (42). In this state, the C12-PN does not significantly interact with the protein as inferred by the lack of spectroscopic changes.

State c: C12-PN above its CMC. The lipid micelles are the primary units interacting with the protein. We propose an intermediate state where the enzyme is fully associated with the C12-PN, but it remains in the micelle still as a dimer, with weaker interaction between its monomers due to the presence of the lipids (Figure 5c). The micelle here is a protein–lipid comicelle with a much reduced number of lipid monomers, with respect to pure C12-PN micelles. In this case, we observe changes in the tryptophan emission mainly due to the exposure of the tryptophan to a more hydrophobic media (blue shift and increase in intensity), but we do not see changes in the number of particles in the excitation volume from FCS measurements. Our data indicate that the

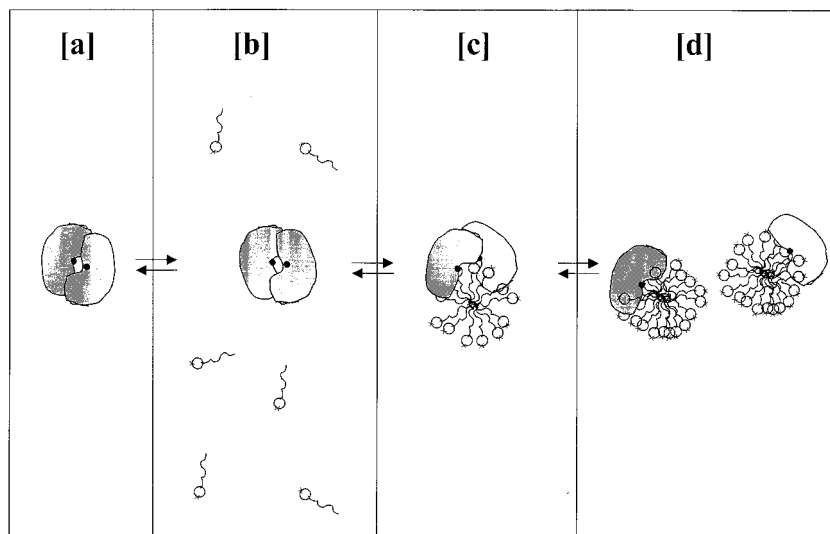


FIGURE 5: Schematic representation of the sequence of events involved in the dissociation of *C. atrox* venom PLA₂ dimer by C12-PN.

changes in tryptophan emission when PLA₂s interact with lipids are due to the interaction with the lipids and not to the dissociation of the dimer. A similar state has also been described for a monomeric PLA₂ porcine pancreas (42, 48, 49).

State d: Excess C12-PN well above its CMC. As more C12-PN is added, changes in the tryptophan spectra (spectral shift and intensity) plateau. At the same time, the migration of PLA₂ monomers to different micelles occurs, as reported by the FCS results (particle number). Each monomer is surrounded by lipids, and no more changes could be observed in tryptophan emission. At these higher C12-PN concentrations the complex diffusion constant, 60 $\mu\text{m}^2/\text{s}$ (55 $\mu\text{m}^2/\text{s}$ in the presence of Ca²⁺), suggests the association of PLA₂ with a large C12-PN micelle. This result indicates that we are observing the association of the PLA₂ monomers with the micelle interface and that the PLA₂ is not (no longer) part of a comicelle.

FCS directly measures the dissociation of the dimer (state d), and tryptophan emission changes are the manifestation of two processes, the association with lipids (state c) and the dissociation of the enzyme (state d). There are two important differences revealed by the tryptophan fluorescence in the presence of calcium. First, with calcium the changes in tryptophan emission start to occur before 1 mM lipid concentration, indicating that the interaction between the lipids and the protein starts earlier in the presence of Ca²⁺. Second, the number of fluorescent particles in the excitation volume starts to increase when the changes in tryptophan emission have almost finished, indicating that calcium stabilizes the intermediate state (state c in our model). Lipids are competing for the monomer interface. It would be reasonable to assume that a tighter dimer would require a higher lipid concentration for dimer dissociation. With this in mind, our results (Figure 4) would indicate that Ca²⁺ increases the affinity of the dimer subunits and stabilizes the intermediate state (state c).

In summary, we have used tryptophan fluorescence and FCS to study the behavior of *C. atrox* PLA₂. By combining both techniques, we gain complementary information. FCS directly monitors the dissociation process of the PLA₂ dimer while changes in tryptophan emission reflect binding of lipid

to PLA₂. In solution the *C. atrox* venom PLA₂ is a tight dimer with a dissociation constant at or below 0.01 nM, either in the presence or in the absence of Ca²⁺ cofactor (Table 1). In the presence of the lipid analogue C12-PN two distinct states can be described: one in which a protein and lipid comicelle form and a second in which the interaction appears to be more in the nature of interfacial binding of the enzyme to an intact C12-PN micelle. The relevant point in terms of PLA₂ activity is the clear indication that the PLA₂ is monomeric at high lipid concentrations. We observed a condition at C12-PN concentrations of 20 mM in which single PLA₂ subunits are bound to individual micelles of C12-PN. It is well documented that PLA₂ is highly active against mixed micellar substrates, such as the Triton X-100 and egg phosphatidylcholine assay system used here. It seems likely that substrate mixed micelles and C12-PN micelles would act toward PLA₂ in a similar fashion. Thus, our observation that the nonhydrolyzable substrate analogue C12-PN dissociates a dimeric PLA₂ supports the single enzyme hypothesis for PLA₂ action on organized lipid substrate.

ACKNOWLEDGMENT

The authors dedicate this work to the memory of Professor Gregorio Weber (1916–1997).

REFERENCES

- Burack, W. R., Dibble, R. G., and Biltonen, R. L. (1997) *Chem. Phys. Lipids* 90, 87–95.
- Hazlett, T. L., Jameson, D. M., Neal, S. E., Webb, M. R., and Eccleston, J. F. (1990) *Biophys. J.* 57, 289a.
- Jain, M. K., Ranadive, G., Yu, B. Z., and Verheij, H. M. (1991) *Biochemistry* 30, 7330–7340.
- Soltys, C. E., and Roberts, M. F. (1994) *Biochemistry* 33, 11608–11617.
- Bell, J. D., and Biltonen, R. L. (1992) *J. Biol. Chem.* 267, 11046–11056.
- Sheffield, M. J., Baker, B. L., Li, D., Owen, N. L., Baker, M. L., and Bell, J. D. (1995) *Biochemistry* 34, 7796–7806.
- Burack, W. R., Yuan, Q., Biltonen, R. L. (1993) *Biochemistry* 32, 583–589.
- Bell, J. D., Baker, M. L., Bent, E. D., Ashton, R. W., Hemming, D. J. B., and Hansen, L. D. (1995) *Biochemistry* 34, 11551–11560.

9. Zidovetzki, R., Laptalo, L., and Crawford, J. (1992) *Biochemistry* 31, 7683–7691.
10. Burack, W. R., and Biltonen, R. L. (1994) *Chem. Phys. Lipids* 73, 209–222.
11. Menashe, M., Romero, G., and Lichtenberg, D. (1986) *J. Biol. Chem.* 261, 5328–5333.
12. Bell, J. D., Brown, S. D., and Baker, B. L. (1992) *Biochim. Biophys. Acta* 1127, 208–220.
13. Ferreira, J. P. M., Sasisekharan, R., Louie, O., and Langer, R. (1994) *Biochem. J.* 303, 527–530.
14. Hille, J. D. R., Egmond, M. R., Dijkman, R., Van Oort, M. G., Jirgensons, B., and De Hass, G. H. (1983) *Biochemistry* 22, 5347–5353.
15. Roberts, M. F., Deems, R. A., and Dennis, E. A. (1977) *Proc. Natl. Acad. Sci. U.S.A.* 74, 1950–1954.
16. Romero, G., Thompson, K., and Biltonen, R. L. (1987) *J. Biol. Chem.* 262, 13476–13482.
17. Welches, W., Reardon, I., and Henrikson, R. L. (1993) *J. Protein Chem.* 12, 187–193.
18. Hazlett, T. L., and Dennis, E. A. (1988) *Biochim. Biophys. Acta* 958, 172–178.
19. Hazlett, T. L., and Dennis, E. A. (1988) *Biochim. Biophys. Acta* 961, 22–29.
20. Bukowski, T., and Teller, D. C. (1986) *Biochemistry* 25, 8024–8033.
21. Kupferberg, J. P., Yokoyama, S., and Kezdy, F. J. (1981) *J. Biol. Chem.* 256, 6274–6281.
22. Hachimori, Y., Wells, M. A., and Hanahan, D. J. (1971) *Biochemistry* 10, 4084–4088.
23. Wells, M. A. (1971) *Biochemistry* 10, 4074–4078.
24. Myatt, E. A., Stevens, F. J., and Sigler, P. B. (1991) *J. Biol. Chem.* 266, 16331–16335.
25. Smith, C. M., and Wells, M. A. (1981) *Biochim. Biophys. Acta* 663, 687–694.
26. Reynolds, L. J., Kempner, E. S., Hughs, L. L., and Dennis, E. A. (1995) *Biophys. J.* 68, 2108–2114.
27. Honger, T., Jorgensen, K., Biltonen, R. L., and Mouritsen, O. G. (1996) *Biochemistry* 35, 9003–9006.
28. Bell, J. D., and Biltonen, R. L. (1989) *J. Biol. Chem.* 264, 225–230.
29. Kilby, P. M., Primrose, W. U., and Roberts, G. C. K. (1995) *Biochem. J.* 305, 935–944.
30. Hazlett, T. L., Johnson, A. E., and Jameson, D. M. (1989) *Biochemistry* 28, 4109–4117.
31. Jameson, D. M., and Hazlett, T. L. (1991) in *Biophysical and Biochemical Aspects of Fluorescence Spectroscopy* (Dewey, T. G., Ed.) pp 105–133, Plenum Publishing Corp., New York.
32. Sanchez, S. A., Hazlett, T. L., Brunet, J. E., and Jameson, D. M. (1998) *Protein Sci.* 7, 2184–2189.
33. Thompson, N. L. (1991) in *Topics in Fluorescence Spectroscopy* (Lakowicz, J. R., Ed.) pp 337–378, Plenum Press, New York.
34. Brunie, S., Bolin, J., Gewirth, D., and Sigler, P. B. (1985) *J. Biol. Chem.* 260, 9742–9749.
35. Jablonski, E. G., Brand, L., and Roseman, S. (1983) *J. Biol. Chem.* 258, 9690–9699.
36. Dennis, E. A. (1973) *J. Lipid Res.* 14, 152–159.
37. Berland, K. M., So, P. T. C., and Gratton, E. (1995) *Biophys. J.* 68, 694–701.
38. Chen, Y., Muller, J. D., Berland, K. M., and Gratton, E. (1999) *Methods* 19, 234–252.
39. Weber, G. (1992) *Proteins Interactions*, Chapman and Hall, New York.
40. Paladini, A. A., and Weber, G. (1981) *Biochemistry* 20, 2587–2593.
41. Santoro, M. M., and Bolen, D. W. (1988) *Biochemistry* 27, 8063–8068.
42. van Dam-Mieras, M. C. E., Slotboom, A. J., Pieterse, W. A., and de Hass, G. H. (1975) *Biochemistry* 14, 5387–5394.
43. Jameson, D. M., and Seifried, S. E. (1999) *Methods* 19, 222–233.
44. Hamman, B. D., Oleinikov, A. V., Jokhadze, G. G., Traut, R. R., and Jameson, D. M. (1996) *Biochemistry* 35, 16680–16686.
45. Keith, C., Feldman, D. S., Deganello, S., Glick, J., Ward, K. B., Jones, E. O., and Sigler, P. B. (1981) *J. Biol. Chem.* 256, 8602–8607.
46. Da Paoian, A. T., Oliveira, A. C., Gaspar, L. P., Silva, J. L., and Weber, G. (1993) *J. Mol. Biol.* 231, 999–1008.
47. Burstein, E. A., Vedenkina, N. S., and Ivkova, M. N. (1973) *Photochem. Photobiol.* 18, 263–279.
48. Soares de Araujo, P., Rosseneu, M. Y., Kremer, J. M. H., van Zoelen, E. J. J., and de Hass, G. H. (1979) *Biochemistry* 18, 580–585.
49. Donne-Op den Kelder, G. M., Hille, J. D. R., Dijkman, R., de Hass, G. H., and Egmond, M. R. (1981) *Biochemistry* 20, 4074–4078.

BI0015991